

Microwave field effects on the time dependence of recombination fluorescence from non-polar solutions

S.V. Anishchik^{a,b}, V.I. Borovkov^a, V.I. Ivannikov^a, I.V. Shebolaev^a,
Yu.D. Chernousov^a, N.N. Lukzen^c, O.A. Anisimov^a, Yu.N. Molin^{a,b}

^a *Institute of Chemical Kinetics and Combustion, 630090 Novosibirsk, Russia*

^b *Novosibirsk State University, 630090 Novosibirsk, Russia*

^c *International Tomography Center, 630090 Novosibirsk, Russia*

Received 10 September 1998; in final form 14 January 1999

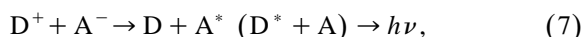
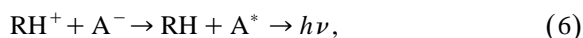
Abstract

A novel experimental setup to study the effect of microwave field on the kinetics of recombination fluorescence from nonpolar solutions irradiated with nanosecond X-ray pulses is described. Experiments on the observation of the microwave field effects in dodecane and hexane solutions are presented. The most favorable conditions for observation of the microwave induced quantum oscillations are found. The effect of spin locking was observed for the first time in the time-resolved microwave field effects. An efficient method to calculate the spin evolution of a radical pair in a microwave field taking into account relaxation is suggested. Analytical expressions for the microwave field effect in the limiting cases of large and small hyperfine splittings are given. © 1999 Elsevier Science B.V. All rights reserved.

1. Introduction

During the recent years new methods using the influence of external magnetic and resonant microwave fields [1–4] and external electric field [5] on the recombination fluorescence have been developed.

Fluorescence from aromatic and other fluorescent compounds added to hydrocarbons has long been used to study spin correlated processes in the radiation spur [2]. The initial ionization and the subsequent reactions can be represented by the following scheme



where RH is the solvent, A and D are the electron and hole acceptors, respectively. These processes form the spin correlated singlet pairs: RH^+/e^- , RH^+/A^- , D^+/e^- and D^+/A^- [2]. Their recombination releases sufficient energy in the solvent, or in the solute if a charge scavenger is added, to produce excited states.

Because of the low dielectric constant of the medium, recombination is mostly geminate, i.e. the positive and negative charges do not separate as far

as the Onsager distance (approx. 30 nm for an alkane at room temperature). For an geminate ion pair two unpaired electrons were initially paired in a molecular singlet state. If recombination is very fast (< 1 ns), this spin correlation is retained, and only singlet products are formed. Over longer periods, the probability of singlet state evolves because of hyperfine interaction between the electrons and magnetic nuclei or due to the difference of g -factors of the recombining partners. The evolution can be disturbed by the resonant microwave pumping. This leads to time-dependent magnetic field and resonant microwave field effects on the product yields, easily detected by studying the fluorescence in suitable systems. The exchange and dipole–dipole interactions do not disturb spin evolution because they are rather weak during the main time of recombination. It is known, that in a real radiation spur the fraction of spin correlated radical ion pairs is less than 100% because of cross-recombination [6–9]. Spin correlation can also be lost due to spin relaxation that randomizes spin orientations. The external magnetic field and resonant microwave field do not effect the recombination fluorescence from uncorrelated pairs.

Nonzero hyperfine interactions or a difference in g -factors of the partners induce transitions between \mathbf{S} and \mathbf{T} levels of system, rendering the initial singlet state of pair non-stationary. As a result, the population of the singlet state changes periodically, modulating the kinetics of recombination fluorescence. These so-called quantum beats have long been observed experimentally [10–12].

Application of a resonant microwave field induces transitions between the \mathbf{T}_0 and \mathbf{T}_+ , as well as between the \mathbf{T}_0 and \mathbf{T}_- triplet levels [13–17]. This also leads to oscillations in the recombination fluorescence. For the first time the microwave induced oscillations were observed in squalane solutions exposed to the 94.6 MHz microwave field [15]. As it had been expected, the experimentally observed frequency of oscillations was proportional to the amplitude of the microwave field B_1 . The frequency of 94.6 MHz corresponds to the resonant field of about 34 G. The low field strength complicated the interpretation of experimental results and, respectively, the developing of the method. Later the oscillations were observed using a time resolved FDMR spectrometer with microwave field frequency of about 10

GHz [17]. The oscillations decayed slower than those reported in the first work [15]. The microwave induced oscillations were also observed during the recombination of neutral radicals in micelles [18].

In the paper [16] a theoretical analysis of spin dynamics under different conditions (external magnetic and microwave fields, hyperfine interactions) based on an exact analytical solution of the problem without spin relaxation was given. Besides the oscillations the other effects, including the effect of spin-locking, were considered.

Compared with the Δg and hfi-induced quantum beats the microwave induced oscillations have not been yet applied for studying of radiation chemistry processes because of a lack of model experiments on simple systems and their adequate theoretical description.

The purpose of the present work was to figure out the optimal conditions for observation of the microwave induced oscillations in the recombination fluorescence and also to study the other microwave induced effects including spin-locking phenomenon. The other purpose was a theoretical analysis of some simple experimental cases.

2. Experimental

The experiments were carried out using nanosecond X-ray fluorimeter [5,19] modified for experiments with microwave field. The schema of the setup is shown in Fig. 1. X-rays pulses of 2 ns generated in a molybdenum target by 40 keV electrons were used for ionization of samples. The light from the sample was passed by quartz lightguide to the photomultiplier tube (PMT). The single photon counting technique was used to record the kinetics. The beam of electrons was passed to the molybdenum target through a hole in the pole of the magnet. A similar hole was also made in the opposite pole to improve the magnetic field homogeneity thus attaining the value better than 1 G. The distance between the target and the sample was about 3 cm.

A rectangular cavity operating at the frequency of about 2.5 GHz in the H_{102} mode was used in the installation. Two special concentrators were assembled inside the cavity to increase B_1 at the sample location (practically double it). To decrease the tran-

sition time, the cavity was overcoupled. The cavity had the coupling coefficient equal to 6, quality factor of about 4000, and the time constant approx. 80 ns.

The microwave power supply system consisted of a reference generator, a solid-state module and a three-stage tube power amplifier. The generator and the solid state module operated continuously, and the power amplifier worked in the pulse regime. The system provided 900 ns microwave pulses at a repetition frequency of 40 kHz. To improve stability of the pulse amplitude, a ferrite isolator was inserted between the generator and the cavity. At the pulse microwave power of 150 W the amplitude B_1 of the microwave magnetic field in the rotating frame was equal to 12 G, the field inhomogeneity over the sample did not exceed 10%. In the laboratory frame of reference the microwave magnetic field is $2B_1 \sin(\omega_0 t + \phi)$.

To improve the signal to noise ratio the signals were accumulated for several hours. The necessary long time magnetic field stability was provided by using a special homebuilt magnet power supply module with NMR-probe feedback. The long time field stability was better than 0.3 G. The resonant field was 883 G for all experiments, which corresponds to the free electron g -factor.

Fig. 2 illustrates the principle of the experiment. The X-ray pulse is switched on after settling of the microwave field amplitude. The amplitude of the

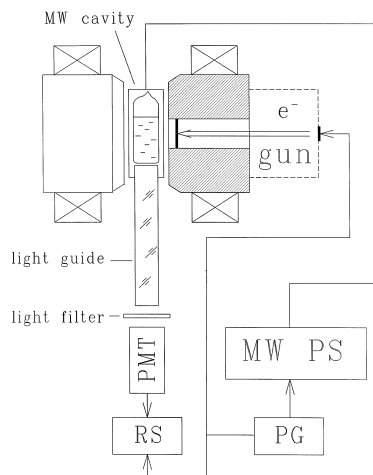


Fig. 1. Block diagram of the apparatus. PG, RS and MW PS stand for the pulse generator, the registration system, and the microwave power supply.

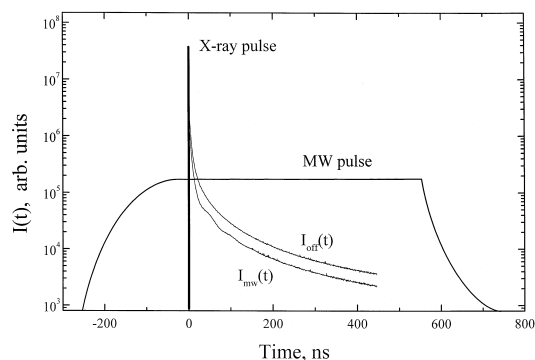


Fig. 2. Scheme of experiment. A MW pulse and an X-ray pulse are schematically shown on the log plot of the recombination fluorescence intensity versus time for n -dodecane solution of 10^{-3} M PTP- d_{14} + 3×10^{-3} M C_6F_6 with microwave field on ($I_{mw}(t)$, $B_1 = 10$ G) and off ($I_{off}(t)$). The curve $I_{off}(t)$ is shifted vertically. Microwave field induced oscillations are seen on the curve $I_{mw}(t)$.

field remains constant during registration time. The microwave field pulses are repeated at a rate of 40 thousand pulses per second. The X-ray pulses rate is twice higher (80 thousand pulses per second). This allows to alternate the light registration with and without microwave field to increase the stability of measurements.

The solvents used (Aldrich Chemical Co., Inc.) were treated with $KMnO_4$, stirred with concentrated H_2SO_4 , washed with water and dried over Al_2O_3 . The purity of the solvents was monitored by UV spectrophotometry (the optical density was less than unit at 200 nm). p -Terphenyl- d_{14} (Aldrich, 99%) was used as received. Samples were degassed by repeated freeze-pump-thaw cycles and sealed in thin-walled quartz cuvettes. All experiments were carried out at 283 ± 1 K.

3. Theory

The time dependence of the recombination fluorescence intensity $I(t)$ can be described by the following expression:

$$I(t) = \frac{1}{\tau_f} \int_{-\infty}^t d\xi \Phi(t - \xi) \int_{-\infty}^{\xi} d\eta \exp\left(-\frac{\xi - \eta}{\tau_f}\right) \times \int_{-\infty}^{\eta} G(\zeta) f(\eta - \zeta) \rho_{ss}(\eta - \zeta) d\zeta, \quad (8)$$

where τ_f , $\Phi(t)$, $G(t)$, and $f(t)$ are the fluorescence lifetime, the setup response function, the function of generation of radical ion pairs, and the recombination kinetics, respectively, and $\rho_{ss}(t)$ is the time dependence of the singlet state population which depends on external magnetic and microwave fields.

The recombination kinetics $f(t)$ is a complicated function that can not be calculated analytically. It depends on many unknown factors. However, in nonpolar solutions $f(t)$ does not depend on magnetic and microwave fields since it does not depend on the pair multiplicity because of a high exothermicity of the reaction of recombination. Therefore it is only the dependence of $\rho_{ss}(t)$ on magnetic and microwave fields that is responsible for magnetic and microwave field effects in the recombination fluorescence.

Assuming that the time resolution of the setup is high enough and fluorescence lifetime τ_f is short the next equation is valid:

$$I(t) \approx f(t) \rho_{ss}(t). \quad (9)$$

Correspondingly the microwave field effect can be represented as:

$$\begin{aligned} \chi(t) &= \frac{I_{\text{mw}}(t) - I_{\text{off}}(t)}{I_{\text{off}}(t)} \\ &= \frac{I_{\text{mw}}(t)}{I_{\text{off}}(t)} - 1 \approx \frac{\rho_{ss}^{\text{mw}}(t)}{\rho_{ss}^{\text{off}}(t)} - 1, \end{aligned} \quad (10)$$

where $I_{\text{mw}}(t)$ and $I_{\text{off}}(t)$ are the recombination fluorescence intensity with and without microwave field, respectively.

Let us consider a germinate radical ion pair that consists of particles A and B . The population $\rho_{ss}(t)$ of the singlet state of the pair can be expressed using spin operators $\hat{S}^A(t)$ and $\hat{S}^B(t)$ of the radicals A and B :

$$\rho_{ss}(t) = \frac{1}{4} - \text{Tr}[\hat{S}^A(t)\hat{S}^B(t)\rho(0)], \quad (11)$$

where $\hat{S}^A(t)$ and $\hat{S}^B(t)$ are generalizations of the Heisenberg representation of spin operators in the presence of relaxation. $\hat{S}_i^{A,B}(0) = \frac{1}{2}\sigma_i$ for $i = x, y, z$, where σ_i are the Pauli matrices. The time evolution of $\hat{S}^A(t)$ can be described in rotating (with mi-

crowave field frequency) frame of reference by the modified Bloch equations (see Appendix A):

$$\begin{aligned} \frac{d}{dt}\hat{S}_x^A &= -\Delta\omega_A\hat{S}_y^A - \frac{1}{T_2^A}\hat{S}_x^A, \\ \frac{d}{dt}\hat{S}_y^A &= \Delta\omega_A\hat{S}_x^A - \omega_1\hat{S}_z^A - \frac{1}{T_2^A}\hat{S}_y^A, \\ \frac{d}{dt}\hat{S}_z^A &= \omega_1\hat{S}_y^A - \frac{1}{T_1^A}\hat{S}_z^A, \end{aligned} \quad (12)$$

where $\omega_1 = \gamma B_1$ ($\gamma = 1.761 \times 10^7$ radianG⁻¹s⁻¹ – gyromagnetic ratio), $\Delta\omega_A$ is frequency detuning of a hfi-component of radical A from the resonance frequency, T_1^A and T_2^A are spin-lattice and spin-spin relaxation times, respectively. The z -axis is parallel to the external magnetic field, the x -axis is aligned with B_1 . The time evolution of $\hat{S}^B(t)$ is described by a similar equations where A is substituted for B .

If the initial state of a radical ion pair is pure singlet (i.e. $\rho_{ss}(0) = 1$ and $\rho_{ik} = 0$ for all $ik \neq ss$), the next equation holds true:

$$\text{Tr}(\rho(0)\hat{S}_i^A(0)\hat{S}_j^B(0)) = -\frac{1}{4}\delta_{ij}, \quad (i, j = x, y, z) \quad (13)$$

where δ_{ij} is the Kronecker symbol.

Let $\Delta\omega_{AB}$ denote the difference of the resonant frequencies of the particles A and B . If particle A is in exact resonance with the microwave field, two extreme cases are possible: the large splitting case ($\Delta\omega_{AB} \gg \omega_1$) and the small splitting case ($\Delta\omega_{AB} \ll \omega_1$).

3.1. $\Delta\omega_{AB} \gg \omega_1$

The probability to be in the singlet state (see Appendix B) is equal to:

$$\begin{aligned} \rho_{ss}^{\text{mw}}(t) &= \frac{1}{4} + \frac{1}{4}\exp(-t/T_1^B) \\ &\quad \times \exp(-t(1/T_1^A + 1/T_2^A)/2) \\ &\quad \times \left(\cos(Zt) + \frac{1/T_2^A - 1/T_1^A}{2Z} \sin(Zt) \right), \end{aligned} \quad (14)$$

where $Z = \sqrt{\omega_1^2 - \frac{1}{4}(1/T_2^A - 1/T_1^A)^2}$, T_1^A and T_1^B are spin-lattice relaxation times for particles A and

B , and T_2^A is spin-spin relaxation time of A . For small values of ω_1 the frequency Z becomes imaginary. There are no oscillations in $\rho_{ss}^{mw}(t)$ in this case.

The probability to be in the singlet state without microwave field is equal to [20]:

$$\rho_{ss}^{off}(t) = \frac{1}{4} + \frac{1}{4}\exp(-t/T_1^B)\exp(-t/T_1^A) \quad (15)$$

The microwave field effect can be described as:

$$\chi(t) = \frac{\Theta[\rho_{ss}^{mw}(t) - \rho_{ss}^{off}(t)]}{\frac{1}{4}(1 - \Theta) + \Theta\rho_{ss}^{off}(t)}, \quad (16)$$

where Θ is the fraction of spin correlated pairs. Eq. (16) takes into account that for noncorrelated pairs the probability of being in the singlet state is equal to $\frac{1}{4}$.

The above equations show that $\chi(t)$ does not depend on $\Delta\omega_{AB}$ in the high splitting case. This means that they are valid for a multiline spectrum of radical B if the requirements of the high splitting case are fulfilled for each line.

3.2. $\Delta\omega_{AB} \ll \omega_1$

The probability for a pair to be in the singlet state in a microwave field is equal to (see Appendix B):

$$\begin{aligned} \rho_{ss}^{mw}(t) = & \frac{1}{4} + \frac{1}{4}\exp(-(1/T_2^A + 1/T_2^B)t) \\ & + \frac{1}{2}\exp(-t[1/T_1^A + 1/T_2^A + 1/T_1^B \\ & + 1/T_2^B]/2). \end{aligned} \quad (17)$$

The probability for a pair to be in the singlet state without microwave field is equal to [20]:

$$\begin{aligned} \rho_{ss}^{off}(t) = & \frac{1}{4} + \frac{1}{4}\exp(-(1/T_1^A + 1/T_1^B)t) \\ & + \frac{1}{2}\exp(-(1/T_2^A \\ & + 1/T_2^B)t)\cos(\Delta\omega_{AB}t). \end{aligned} \quad (18)$$

The case of small splitting is also realized if both lines are inhomogeneous broadened and the following inequality for the second moments Δ_A^2 and Δ_B^2 of the ESR spectra of partners is valid: $\Delta_A^2 + \Delta_B^2 \ll \omega_1^2$.

In this case the probability for a pair to be in the singlet state in a microwave field is described by Eq.

(17). In the absence of microwave field this probability is equal to [20]:

$$\begin{aligned} \rho_{ss}^{off}(t) = & \frac{1}{4} + \frac{1}{4}\exp(-(1/T_1^A + 1/T_1^B)t) \\ & + \frac{1}{2}\exp(-t^2(\Delta_A^2 + \Delta_B^2)/2) \\ & \times \exp(-(1/T_2^A + 1/T_2^B)t)\cos(\Delta\omega t), \end{aligned} \quad (19)$$

where $\Delta\omega$ is the splitting between lines that belong to A and B .

Fig. 3 shows results of some calculations of the microwave field effect for the case of large splitting. As one can see, the time dependence of the effect can be represented as a sum of two functions: an oscillating one (with decaying amplitude of oscillations) and a negative monotonous function also vanishing with time. A variation of parameters shows that the decay of the monotonous function depends on the spin-lattice relaxation times T_1^A and T_1^B of the recombining radical ions, but decay of the oscillations depends mainly on the phase relaxation of radical A .

Fig. 4 shows the results of calculations for the case of small splitting. As one can see in this case there are no oscillations. The time evolution of the microwave field effect depends on spin-relaxation

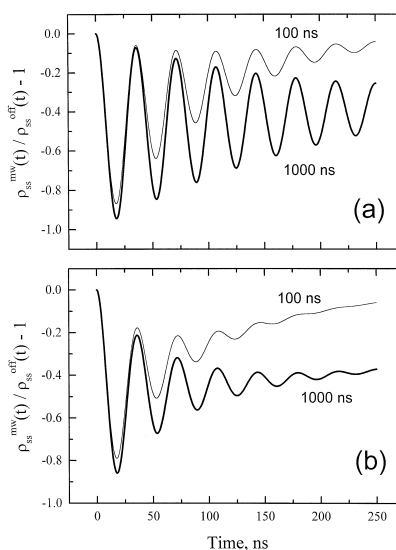


Fig. 3. The calculated microwave field effect for the large splitting case for the parameters: $B_1 = 10$ G, $T_1^A = 1000$ ns, $T_2^A = 100$ ns (a), $T_2^A = 30$ ns (b). The values of T_1^B are shown next to the curves.

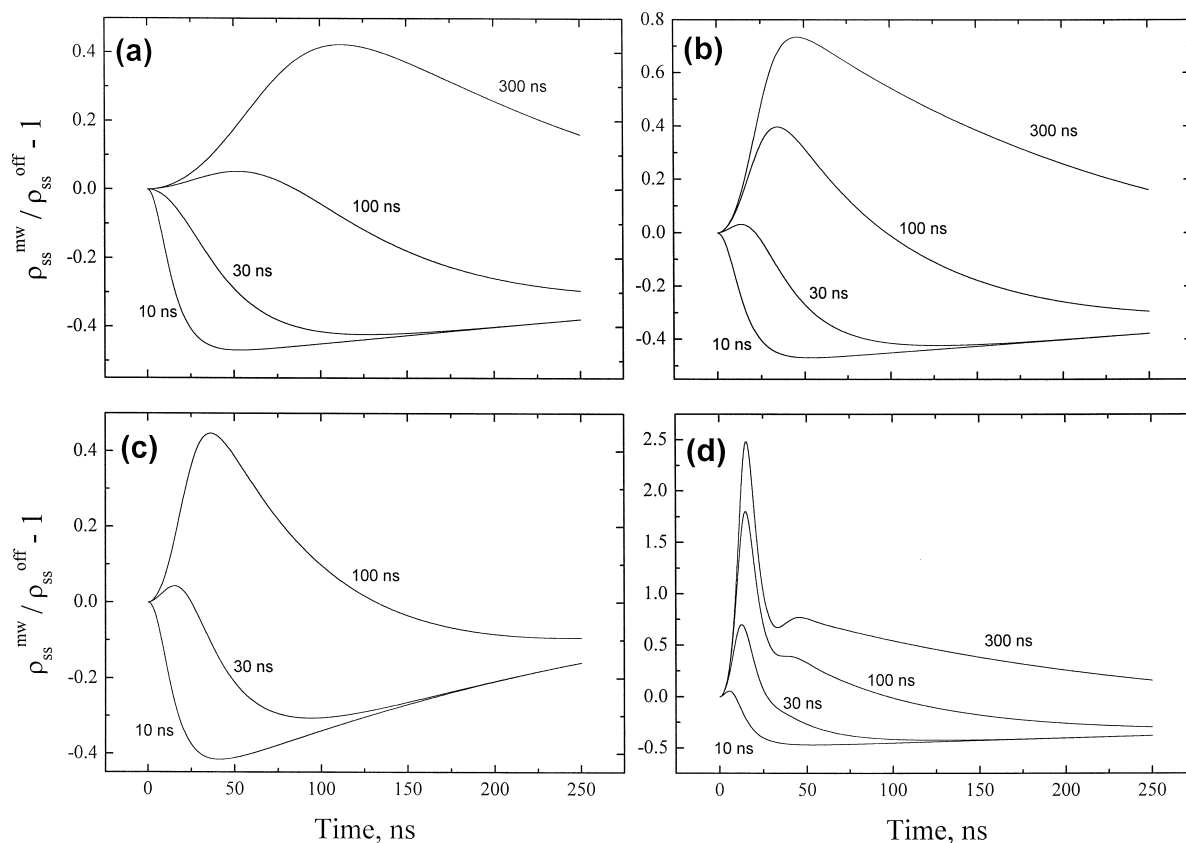


Fig. 4. The calculated microwave field effect for the small splitting case for $T_1^A = T_1^B = T_1$, $T_2^A = T_2^B = T_2$, $\Delta_A^2 = \Delta_B^2 = \Delta^2$. (a) $T_1 = 1000$ ns, $\Delta^2 = 1$ G², $\Delta\omega = 0$, (b) $T_1 = 1000$ ns, $\Delta^2 = 10$ G², $\Delta\omega = 0$, (c) $T_1 = 300$ ns, $\Delta^2 = 10$ G², $\Delta\omega = 0$, (d) $T_1 = 1000$ ns, $\Delta^2 = 10$ G², $\Delta\omega = 10$ G. The values of T_2 are shown next to the curves.

times. If both T_1 and T_2 are long enough the spin-locking phenomenon is observed (the transitions between **S** and **T**₀ levels of the pair are slowed by strong microwave field). The curve of the microwave field effect for this case remains positive all the time. As T_2^A and T_2^B become shorter, the curves become bipolar or (for the shortest times) even negative. The steepness of rising and lowering of the curves and the amplitudes of the extrema increase if the inhomogeneous width of ESR spectra of radical ions and/or $\Delta\omega$ splitting increase. If both of the latter factors are big (Fig. 4(d)) some oscillations appear.

4. Results and discussion

As was mentioned above, the large splitting case is most favorable for observation of microwave field

induced quantum oscillations. It is realized if the width of the ESR spectrum of one of the radical ions is less than B_1 but the width of the spectrum of another partner significantly exceeds it. In this case the microwave field effects the spins of all the first partners but has practically no effect on the spins of the second ones. On the other hand the efficiency of **S**–**T**₀ transitions is rather high in this situation.

To realize these conditions we chose the solution of PTP-*d*₁₄ and C₆F₆ in n-dodecane. The second moments of the ESR spectra of radical cation and anion of PTP-*d*₁₄ are less than 1 G². The ESR spectrum of radical anion of C₆F₆ is broad due to the splitting of 135 G on the 6 equivalent fluorine nuclei. The C₆F₆ molecules have a positive electron affinity and rather high ionization potential. Therefore they can capture electrons but can not capture holes. So

the pairs that recombine in aforementioned system are mainly $C_6F_6^-$ and $PTP-d_{14}^+$ or $C_6F_6^-$ and the solvent hole RH^+ . As it will be shown below the ESR spectrum of RH^+ is also rather narrow. If the concentrations of C_6F_6 and $PTP-d_{14}$ are comparable, recombining pairs of another type ($PTP-d_{14}^-$ and $PTP-d_{14}^+$) can also be formed because of a competition for electron capture.

Fig. 5 shows the time resolved microwave field effect for the solutions of $PTP-d_{14}$ and C_6F_6 in n-dodecane for different concentrations of C_6F_6 . All curves except curve 3 are shifted along vertical axis for better presentation (all original curves are started at zero).

For a correct analysis of experimental curves it is essential to bear in mind that the amplitude of noise on the curves monotonously increases with time. The reason for this is that it is proportional to the square root of light intensity. Since $f(t) \propto t^{-3/2}$ for the most part of time scale, the amplitude of noise is proportional to $t^{3/4}$ and increases with time.

As one can see from Fig. 5 the experimental curves are similar to the calculated ones (see Fig. 3). The time dependence of microwave field effect can be represented as a sum of two functions: an oscillating one (with decaying amplitude of oscillations) and a negative monotonous function also decaying with time. Its decay time decreases with increasing the concentration of C_6F_6 . In the same way the decay

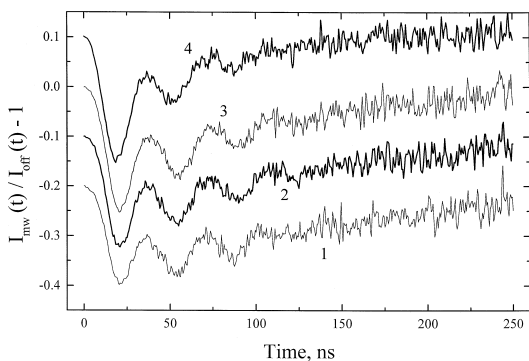


Fig. 5. Experimentally observed microwave field effect in the recombination fluorescence for n-dodecane solutions: 10^{-3} M $PTP-d_{14}$ + 3×10^{-3} M C_6F_6 (1), 6×10^{-3} M C_6F_6 (2), 10^{-2} M C_6F_6 (3), 3×10^{-2} M C_6F_6 (4). $B_1 = 10$ G. All curves (except (3)) are shifted vertically. For all curves the effect is equal to zero at $t = 0$.

time of oscillations decreases. At the concentration of C_6F_6 equal to 3×10^{-3} M the decay time of the monotonous function is about 150 ns and the decay time of oscillations is equal to approximately 50 ns. Their difference decreases when the concentration of C_6F_6 is increased, and the times reach the values of 50 and 40 ns, respectively.

The decay of both the monotonous function and the oscillations should depend on phase relaxation of the positive partner of the pair and on spin-lattice relaxation of both recombining particles. Phase relaxation of the hexafluorobenzene radical anion has a much weaker effect.

The concentration dependence of decay time has its origin in the charge transfer reaction between a radical anion and a neutral molecule of C_6F_6 that decreases the spin-lattice relaxation time of the radical anion when the concentration of C_6F_6 is increased [10,21]. The analytical calculation of the relaxation time is difficult because the high field approximation is not applicable here (the width of the ESR spectrum of the radical anion is comparable with the magnitude of external magnetic field).

The amplitude of the effect decreases if the concentration of C_6F_6 is decreased. This is because of an increasing fraction of the pairs $PTP-d_{14}^- - PTP-d_{14}^+$ and $PTP-d_{14}^- - RH^+$ (where RH^+ is the solvent hole) at low concentration of C_6F_6 . Since both partners of these pairs have narrow ESR spectra, their contribution to the total signal is positive, corresponding to the spin-locking case (see Fig. 4). Therefore the amplitude of the total signal at short times becomes smaller.

Figs. 6–9 show the experimental microwave field effects for different situations that have been theoretically considered earlier. The experiments were carried out with n-hexane solutions containing $PTP-d_{14}$ and different alkanes. n-Hexane was chosen as a solvent because of its high ionization potential (10.13 eV) that allows to use various alkanes as hole acceptors. Since alkanes have negative electron affinity, in all experiments the negative partner was the radical anion of $PTP-d_{14}$ (and partly uncaptured electron).

Fig. 6 shows the microwave field effect for the solution of 10^{-3} M $PTP-d_{14}$ in n-hexane. At short times the behavior of the curve is similar to one shown in Fig. 5 but there are practically no oscillations, the signal just quickly vanishes. Since the

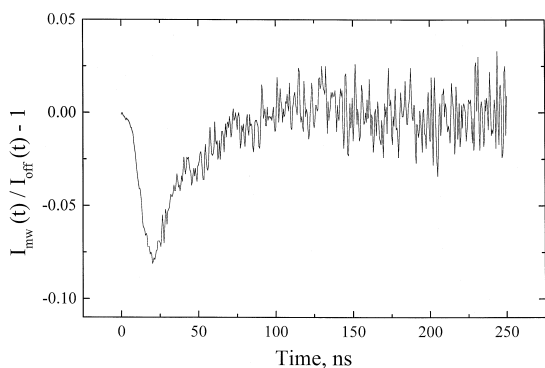


Fig. 6. Experimentally observed microwave field effect in the recombination fluorescence for the solution of 10^{-3} M PTP- d_{14} in n-hexane. $B_1 = 10$ G.

initial slope of the curve is high one can conclude that one of partners has a wide ESR spectrum and the curve should oscillate (see the results of calculations in Fig. 3). The lack of oscillations is probably due to fast capture of radical cations by PTP- d_{14} . This is confirmed by the equality of the decay time (about 50 ns) and the time of the solvent radical cation capture by PTP- d_{14} . The diffusion controlled rate constant of the latter process is about $2 \times 10^{10} \text{ M}^{-1} \text{ s}^{-1}$. The corresponding time of solvent radical cation capture is estimated to be about 50 ns.

The next experiment was carried out with isooctane solution (see results in Fig. 7). In this case one

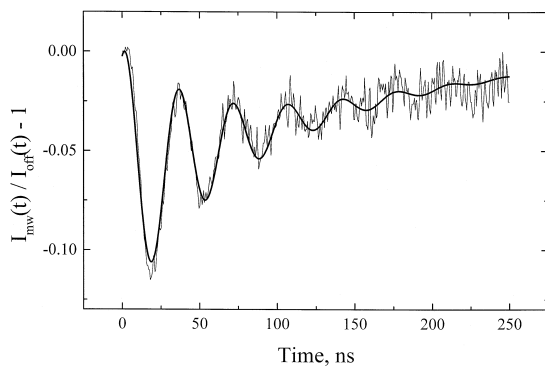


Fig. 7. Experimentally observed microwave field effect in the recombination fluorescence for the solution of 3×10^{-5} M PTP- d_{14} + 5×10^{-1} M of isooctane in n-hexane at $B_1 = 10$ G (noisy thin line). Calculated microwave field effect for the following values of parameters: $T_1^A = 974$ ns, $T_2^A = 39$ ns, $T_1^B = 149$ ns, $B_1 = 10.2$ G, $\theta = 0.18$, the time shift is equal to 1.5 ns (thick line).

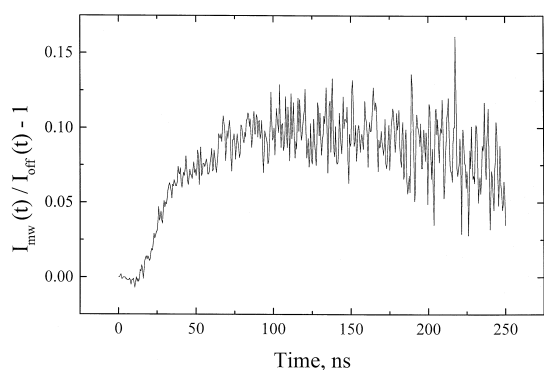


Fig. 8. Experimentally observed microwave field effect in the recombination fluorescence for the solution of 10^{-3} M PTP- d_{14} + 10^{-1} M of n-dodecane in n-hexane. $B_1 = 10$ G.

can expect the favorable conditions for observation of the oscillations because, as we discovered earlier [9], the radical cation of isooctane (or the product of its transformation) has a broad ESR spectrum. The concentration of PTP- d_{14} was chosen very low to preclude the transfer of positive charge from isooctane $^+$ to *para*-terphenyl. The curve in Fig. 7 is similar to that in Fig. 5 but the magnitude of the effect is smaller and the decay time is longer. For the radical cation of isooctane the reaction of ion-molecular charge transfer has less effect on spin-lattice relaxation time than for the C_6F_6 radical anion because of the smaller width of its ESR spectrum as compared to that for the latter.

Fig. 7 also shows the least square fit of the experimental curve using equations (14)–(16). The

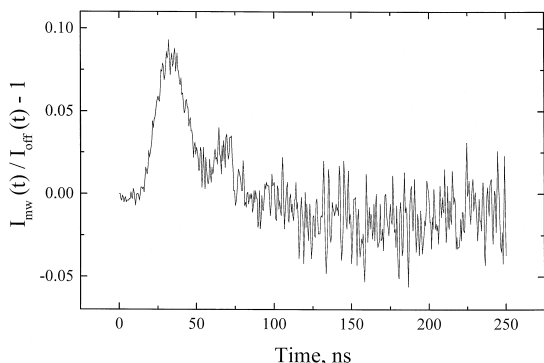


Fig. 9. Experimentally observed microwave field effect in the recombination fluorescence for the solution of 10^{-4} M PTP- d_{14} + 10^{-1} M of n-dodecane in n-hexane. $B_1 = 10$ G.

calculated curve was shifted to the right by 1.5 ns, which is close to the fluorescence lifetime of PTP- d_{14} . The varied parameters included the spin-lattice and spin-spin relaxation times, the microwave field strength B_1 and a normalizing factor for $\chi(t)$ to take into account the fraction of spin-correlated pairs. The best fitting values of parameters are given in figure captions. The low values of T_2^A and the normalizing coefficient can be attributed to the charge transfer reaction between a radical cation and a neutral molecule of isooctane. Because of this exchange the spin of the positive partner can multiply pass through the resonant microwave field. This leads to a decrease in T_2^A and the amplitude of the microwave field effect.

Figs. 8 and 9 show the experimental curves of the microwave field effect in n-hexane solutions of 10^{-1} M n-dodecane and different concentrations of PTP- d_{14} : 10^{-3} M – Fig. 8 and 10^{-4} M – Fig. 9. As one can expect the figures demonstrate the phenomenon of spin-locking like the theoretical curves show in Fig. 4. Unlike the isooctane case it occurs because the radical cation of n-dodecane has a narrow ESR spectrum. The decay time of the effect depends on the concentration of PTP- d_{14} . At high concentration (Fig. 8) the decay is rather slow. At low concentration (Fig. 9) the decay is faster and small oscillations are noticeable. The difference is probably due to the charge transfer reaction between an n-dodecane radical cation and a PTP- d_{14} molecule that can occur at concentration of 10^{-3} M PTP- d_{14} .

At low concentration (Fig. 9) the radical cation of PTP- d_{14} does not participate in spin evolution and the decay becomes faster. The appearance of oscillation indicates that width of the ESR spectrum of n-dodecane radical cation is larger than that of PTP- d_{14} but it remains small enough to provide spin-locking.

5. Conclusion

The high sensitivity of the microwave field effects to the relaxation times of radical ions and to the parameters of their ESR spectra makes them rather promising for study of primary radical ions under ionization of solutions.

Acknowledgements

Financial support from the Russian Foundation for Basic Research, grant 97-03-32503a, the Foundation ‘‘Russian Universities’’, grant 3524/3H-315-98, and the Foundation ‘‘Leading Groups Program’’, grant 15-97564 is gratefully acknowledged.

Appendix A

The singlet state population $\rho_{ss}(t)$ can be described using spin operators \hat{S}^A and \hat{S}^B of radical ions A and B :

$$\rho_{ss}(t) = \frac{1}{4} - \text{Tr}[\hat{S}^A \hat{S}^B \rho(t)], \quad (\text{A.1})$$

where $\rho(t)$ is density matrix of radical pair (RP), $\hat{S}_i^{A,B} = \frac{1}{2} \hat{\sigma}_i$, $\hat{\sigma}_i$ is the Pauli matrix, $i = x, y, z$.

Ignoring dipole–dipole and exchange interactions of spins one can calculate the dynamics for each spin separately and then determine $\rho(t)$. This is rather simple if the density matrix $\rho(0)$ at zero time can be described as a Cartesian product of matrices ρ^A and ρ^B (related solely to the spins A and B , respectively). Unfortunately, it is often impossible to apply this approach directly (in particular for singlet initial state of the pair). Below we will show how to overcome this difficulty.

For the average values of spin projections $\langle S_i^A \rangle$ one can write the Bloch equations:

$$\begin{aligned} \frac{d}{dt} \langle S_x^A \rangle &= -\Delta \omega_A \langle S_y^A \rangle - \frac{1}{T_2^A} \langle S_x^A \rangle, \\ \frac{d}{dt} \langle S_y^A \rangle &= \Delta \omega_A \langle S_x^A \rangle - \omega_1 \langle S_z^A \rangle - \frac{1}{T_2^A} \langle S_y^A \rangle, \\ \frac{d}{dt} \langle S_z^A \rangle &= \omega_1 \langle S_y^A \rangle - \frac{1}{T_1^A} \langle S_z^A \rangle. \end{aligned} \quad (\text{A.2})$$

The $\langle \rangle$ means the averaging over the density matrix $\rho^A(t)$ of spin A :

$$\langle S_i^A \rangle = \text{Tr}[S_i^A \rho^A(t)].$$

Eqs. (A.2) describe the spin evolution in crossed magnetic and microwave fields. The direction of the magnetic field is along the z -axis. The direction of the magnetic component of microwave field is along

the x -axis in the rotating frame and its amplitude is equal to ω_1 . In Eq. (A.2), $\Delta\omega_A$ is the difference between the frequency of spin precession (for a given hfi-component of the ESR spectrum of radical A) and the resonance frequency, T_1^A, T_2^A are spin-lattice and spin-spin relaxation times, respectively. The same equations can be written for spin B (substituting in (A.2) A for B).

Let us introduce operators $\hat{\eta}_i^A$ and $\hat{\eta}_k^B$ in the next way:

$$\hat{\eta}_0^{A,B} = \frac{1}{2}\mathbf{E}; \quad \hat{\eta}_q^{A,B} = \hat{S}_q^{A,B} = \frac{1}{2}\hat{\sigma}_q, \quad q = x, y, z,$$

where \mathbf{E} is the unitary matrix.

Now we will consider the evolution of the average values of the operators $\hat{\eta}_i^A$ and $\hat{\eta}_k^B$. The solution for $\langle \hat{\eta}_0^{A,B} \rangle(t)$ is quite clear:

$$\langle \hat{\eta}_0^{A,B} \rangle(t) = \langle \hat{\eta}_0^{A,B} \rangle(t=0).$$

To find the average values of the operators $\hat{\eta}_q^{A,B}$, $q = x, y, z$ one should solve the Bloch equations (A.2) for spins A and B .

Because Eqs. (A.2) are linear, one can write for $\langle \hat{\eta}_i^{A,B} \rangle(t)$:

$$\begin{aligned} \langle \hat{\eta}_i^A \rangle(t) &= \sum_n A_{in}(t) \langle \hat{\eta}_n^A \rangle(0), \\ \langle \hat{\eta}_k^B \rangle(t) &= \sum_m B_{km}(t) \langle \hat{\eta}_m^B \rangle(0), \end{aligned} \quad (\text{A.3})$$

where $A_{0n} = \delta_{0n}$, $B_{0m} = \delta_{0m}$, δ_{ij} is the Kronecker symbol.

Let us choose the matrix $\hat{\eta}_n^A$ as the initial density matrix for spin A . Then the average value of some operator $\hat{\eta}_i^A$ at $t=0$ is equal to $\langle \hat{\eta}_i^A \rangle(0) = \text{Tr}(\hat{\eta}_i^A \hat{\eta}_n^A) = \frac{1}{4}\delta_{in}$. Taking into account (A.3) one can write:

$$\langle \hat{\eta}_i^A \rangle(t) = \frac{1}{4}A_{in}(t). \quad (\text{A.4})$$

On the other hand if the evolution of spin A is described by the Liouvillian \hat{L}_A :

$$\frac{d}{dt}\rho^A(t) = \hat{L}_A \rho^A(t) \Rightarrow \rho^A(t) = e^{L_A t} \rho^A(0),$$

then (taking into account that $\rho^A(0) = \eta_n^A$) one can write:

$$\langle \hat{\eta}_i^A \rangle(t) = \text{Tr}(\hat{\eta}_i^A \rho^A(t)) = \text{Tr}(\hat{\eta}_i^A e^{L_A t} \hat{\eta}_n^A). \quad (\text{A.5})$$

Comparing (A.4) and (A.5) and substituting A for B in all expressions we have:

$$\begin{aligned} A_{in}(t) &= 4 \text{Tr}(\hat{\eta}_i^A e^{L_A t} \hat{\eta}_n^A), \\ B_{km}(t) &= 4 \text{Tr}(\hat{\eta}_k^B e^{L_B t} \hat{\eta}_m^B). \end{aligned} \quad (\text{A.6})$$

We will now consider how to determine the average value of the operator $\hat{\eta}_i^A \hat{\eta}_k^B$ in more general case:

$$\langle \hat{\eta}_i^A \hat{\eta}_k^B \rangle(t) = \text{Tr}[\hat{\eta}_i^A \hat{\eta}_k^B \rho(t)],$$

where i and k run through the values $0, x, y, z$. The Liouvillian $\hat{L} = \hat{L}_A + \hat{L}_B$ drives the evolution of the spin density matrix of the radical pair $\rho(t)$ (ignoring interactions of the spins):

$$\rho(t) = e^{L t} \rho(0) = e^{(L_A + L_B)t} \rho(0).$$

Because the products $\hat{\eta}_i^A \hat{\eta}_m^B$ form a full set in the spin space of RP, then *any matrix* $\rho(0)$ can be expanded this way:

$$\rho(0) = \sum_{m,n} C_{mn} \hat{\eta}_m^A \hat{\eta}_n^B,$$

where

$$C_{mn} = 16 \text{Tr}[\hat{\eta}_i^A \hat{\eta}_m^B \rho(0)].$$

As a result for the time evolution of the average values of $\hat{\eta}_i^A \hat{\eta}_k^B$ we can write:

$$\begin{aligned} \langle \hat{\eta}_i^A \hat{\eta}_k^B \rangle(t) &= \sum_{m,n} C_{mn} \text{Tr}[\hat{\eta}_i^A \hat{\eta}_k^B e^{(L_A + L_B)t} \hat{\eta}_m^A \hat{\eta}_n^B] \\ &= \sum_{m,n} C_{mn} \text{Tr}(\hat{\eta}_i^A e^{L_A t} \hat{\eta}_m^A) \text{Tr}(\hat{\eta}_k^B e^{L_B t} \hat{\eta}_n^B) \\ &= \frac{1}{16} \sum_{m,n} C_{mn} A_{in}(t) B_{km}(t) \\ &= \text{Tr} \left[\left(\sum_n A_{in}(t) \hat{\eta}_n^A \right) \left(\sum_m B_{km}(t) \hat{\eta}_m^B \right) \rho(0) \right]. \end{aligned} \quad (\text{A.7})$$

Introducing the initial conditions $\hat{a}_i(0) = \hat{\eta}_i^A$ and $\hat{b}_k(0) = \hat{\eta}_k^B$ for operators

$$\hat{a}_i(t) = \sum_n A_{in}(t) \hat{\eta}_n^A, \quad \hat{b}_k(t) = \sum_m B_{km}(t) \hat{\eta}_m^B,$$

we can write:

$$\hat{a}_i(t) = \sum_n A_{in}(t) \hat{a}_n(0),$$

$$\hat{b}_k(t) = \sum_m B_{km}(t) \hat{b}_m(0) \quad (\text{A.8})$$

and because of (A.7):

$$\langle \hat{\eta}_i^A \hat{\eta}_k^B \rangle(t) = \langle \hat{a}_i(t) \hat{b}_k(t) \rangle$$

$$= \text{Tr} \left[\hat{a}_i(t) \hat{b}_k(t) \rho(0) \right]. \quad (\text{A.9})$$

From the comparison (A.3) and (A.8) one can see a similarity of the equations that describe time evolution of the operators $\hat{a}_i(t)$ and $\hat{b}_k(t)$ and time evolution of the average values $\langle \hat{\eta}_i^A \rangle(t)$ and $\langle \hat{\eta}_k^B \rangle(t)$. For the components $\hat{a}_i(t)$, $\hat{b}_k(t)$, where i and k run through the values x, y, z , equations have the form of the Bloch equations in which the average values $\langle \hat{S}_x^{A,B} \rangle$, $\langle \hat{S}_y^{A,B} \rangle$, $\langle \hat{S}_z^{A,B} \rangle$ are substituted for the operators $\hat{a}_x(t)$, $\hat{a}_y(t)$, $\hat{a}_z(t)$, $\hat{b}_x(t)$, $\hat{b}_y(t)$, $\hat{b}_z(t)$. So we can now generalize the Heisenberg representation to take spin relaxation into account. We postulate that $\hat{S}^A(t) = \hat{a}(t)$ and $\hat{S}^B(t) = \hat{b}(t)$, where $\hat{a}(t)$ and $\hat{b}(t)$ are vectors with operators $\hat{a}_i(t)$, $\hat{b}_k(t)$ (at $i, k = x, y, z$) as components. Then one can consider the operators $\hat{a}_i(t)$ and $\hat{b}_k(t)$ the operators of the spin of the radicals evolving with time.

Taking all this into account we can rewrite (A.1) as formula (11). The evolution of $\hat{S}^A(t)$ and $\hat{S}^B(t)$ is described now by expression (12).

Appendix B

Two limiting cases are possible:

I. $\Delta \omega_{AB} = |\Delta \omega_A - \Delta \omega_B| \gg \omega_1$ and radical A is in resonance.

The solution of the system (12) for spin B with high accuracy is:

$$\hat{S}_x^B(t) = \exp(-t/T_2^B) \left[\hat{S}_x^B(0) \cos(\Delta \omega_B t) \right. \\ \left. + \hat{S}_y^B(0) \sin(\Delta \omega_B t) \right],$$

$$\hat{S}_y^B(t) = \exp(-t/T_2^B) \left[\hat{S}_y^B(0) \cos(\Delta \omega_B t) \right. \\ \left. - \hat{S}_x^B(0) \sin(\Delta \omega_B t) \right],$$

$$\hat{S}_z^B(t) = \exp(-t/T_1^B) \hat{S}_z^B(0). \quad (\text{B.1})$$

Reconstructing the Laplace images from [21] we can write for spin A (that is in resonance):

$$\hat{S}_x^A(t) = \exp(-t/T_2^A) \hat{S}_x^A(0),$$

$$\hat{S}_y^A(t) = \hat{S}_y^A(0) \exp(-t(1/T_1^A + 1/T_2^A)/2) \\ \times \left[\cos(Zt) - \sin(Zt)(1/T_2^A - 1/T_1^A) \right. \\ \left. / (2Z) \right] - \omega_1 \hat{S}_z^A(0) \exp(-t(1/T_1^A \\ + 1/T_2^A)/2) \sin(Zt) / Z,$$

$$\hat{S}_z^A(t) = \hat{S}_z^A(0) \exp(-t(1/T_1^A + 1/T_2^A)/2) \\ \times \left[\cos(Zt) + \sin(Zt)(1/T_2^A - 1/T_1^A) \right. \\ \left. / (2Z) \right] + \omega_1 \hat{S}_y^A(0) \exp(-t(1/T_1^A \\ + 1/T_2^A)/2) \sin(Zt) / Z, \quad (\text{B.2})$$

where $Z = \sqrt{\omega_1^2 - \frac{1}{4}(1/T_2^A - 1/T_1^A)^2}$.

Using (11), (13) and (B.1), (B.2) we get for $\rho_{ss}(t)$:

$$\rho_{ss}(t) = \frac{1}{4} \left\{ 1 + \exp(-t(1/T_2^A + 1/T_2^B)) \right. \\ \times \cos(\Delta \omega_{AB} t) + \exp(-t/T_2^B) \cos(\Delta \omega_{AB} t) \\ \times \left(\cos Zt - \frac{1/T_2^A - 1/T_1^A}{2Z} \sin Zt \right) \\ \times \exp(-t(1/T_1^A + 1/T_2^A)/2) \\ \left. + \exp(-t/T_1^B) \exp(-t(1/T_1^A + 1/T_2^A)/2) \right. \\ \left. \times \left(\cos Zt + \frac{1/T_2^A - 1/T_1^A}{2Z} \sin Zt \right) \right\} \quad (\text{B.3})$$

Practically $\Delta \omega_{AB}^{-1}$ is usually much less than fluorescence lifetime and time resolution of the setup. Therefore the second and third terms in (B.3) become very small and can be omitted. The same simplification is valid for short T_2^B . As a result we can use a more simple formula (14).

II. $|\Delta \omega_A| \ll \omega_1$, $|\Delta \omega_B| \ll \omega_1$ and $|\Delta \omega_{AB}| \ll \omega_1$ and both spins are close to resonance.

In this case one can use the solutions of (B.2) assuming $\omega_1 \rightarrow \infty$. Using also (13) we get:

$$\rho_{ss} = \frac{1}{4} + \frac{1}{4} \exp(-t(1/T_2^A + 1/T_2^B)) \\ + \frac{1}{2} \exp(-t[1/T_1^A + 1/T_2^A + 1/T_1^B \\ + 1/T_2^B]/2). \quad (\text{B.4})$$

As one can see here $\rho_{ss}(t)$ does not depend on ω_1 , and the population $\rho_{ss}(t) \rightarrow \frac{1}{4}$ with the time which is determined by T_2^A and T_2^B , and not by T_1^A and T_1^B , which is the case when there is no microwave field.

References

- [1] B. Brocklehurst, Nature 221 (1969) 921.
- [2] B. Brocklehurst, Intern. Rev. Phys. Chem. 4 (1985) 279.
- [3] U.E. Steiner, T. Ulrich, Chem. Rev. 89 (1989) 51.
- [4] K.M. Salikhov, Yu.N. Molin, R.Z. Sagdeev, A.L. Buchachenko, Spin polarization and magnetic effects in radical reactions, Yu.N. Molin (Ed.), Elsevier, Amsterdam, 1984.
- [5] V.I. Borovkov, S.V. Anishchik, O.A. Anisimov, Chem. Phys. Letters 270 (1997) 327.
- [6] G.I. Baker, B. Brocklehurst, I.R. Holton, Chem. Phys. Letters 134 (1987) 83.
- [7] B. Brocklehurst, Chem. Phys. Letters 211 (1993) 31.
- [8] J.A. LaVerne, B. Brocklehurst, J. Phys. Chem. 100 (1996) 1682.
- [9] S.V. Anishchik, O.M. Usov, O.A. Anisimov, Yu.N. Molin, Radiat. Phys. Chem. 51 (1998) 31.
- [10] J. Klein, R. Voltz, Phys. Rev. Letters 36 (1976) 1214.
- [11] O.A. Anisimov, V.L. Bizyaev, N.N. Lukzen, V.M. Grigoryants, Yu.N. Molin, Chem. Phys. Letters 101 (1983) 131.
- [12] A.V. Veselov, V.I. Melekhov, O.A. Anisimov, Yu.N. Molin, Chem. Phys. Letters 136 (1987) 263.
- [13] O.A. Anisimov, V.M. Grigoryants, V.K. Molchanov, Yu.N. Molin, Chem. Phys. Letters 66 (1979) 265.
- [14] A.D. Trifunac, J.P. Smith, Chem. Phys. Letters 73 (1980) 94.
- [15] V.O. Saik, O.A. Anisimov, A.V. Koptyug, Yu.N. Molin, Chem. Phys. Letters 165 (1990) 142.
- [16] K.M. Salikhov, Yu.N. Molin, J. Phys. Chem. 97 (1993) 13259.
- [17] I.A. Shkrob, A.D. Trifunac, J. Chem. Phys. 103 (1995) 551.
- [18] B.M. Tadjikov, A.V. Astashkin, Y. Sakaguchi, Chem. Phys. Letters 283 (1998) 179.
- [19] S.V. Anishchik, V.M. Grigoryants, V.M. Shebolaev, Yu.D. Chernousov, O.A. Anisimov, Yu.N. Molin, Pribory i tekhnika eksperimenta, 1989, No. 4, p. 74, in Russian.
- [20] V.A. Bagryansky, O.M. Usov, N.N. Lukzen, Yu.N. Molin, Appl. Magn. Reson. 12 (1997) 505.
- [21] V.O. Saik, N.N. Lukzen, V.M. Grigoryants, O.A. Anisimov, A.B. Doktorov, Yu.N. Molin, Chem. Phys. 84 (1984) 421.